COBEM 2023 27TH INTERNATIONAL CONGRESS OF MECHANICAL ENGENEERING

ABCM Brazilian Society of Mechanical Sciences and Engineering
27th ABCM International Congress of Mechanical Engineering
December 04-08, 2023, Florianópolis-SC, Brazil

COB-2023-1385
ALUMINA AND ZIRCONIA COMPOSITE FILAMENTS FOR 3D PRINTING OF SCAFFOLDS BY FUSED FILAMENT FABRICATION PROCESS

Maíra Faccio
Jadna Catafesta
Janete Eunice Zorzi
Carlos Alberto Costa
University of Caxias do Sul (UCS)
mfaccio1@ucs.br, *jcatafes@ucs.br*, jezorzi@ucs.br, *cacosta@ucs.br*

Abstract. *This work presents the development of a composite filament for the manufacture by 3D printing of alumina and zirconia scaffolds, which were infiltrated with bioglass for application in the biomedical area. The ceramic powders were morphologically evaluated by scanning electron microscopy (SEM). The filaments were obtained in a twin-screw extruder by mixing the ceramic powders (55%wt) and the low-density polyethylene (LDPE) polymer (45%wt). Using the manufactured filaments, an analysis of the filaments was carried out by SEM with subsequent printing of the scaffolds using the FFF process. Thermogravimetric analysis (TGA) was performed to create the degradation curve in a powder bed to remove the polymer from the scaffold. Finally, the scaffolds were evaluated for morphological and physical e properties. The results identified a particle size distribution for alumina between 0.4 - 0.6 μm and zirconia between 0.09 - 0.2 μm. The micrographs of the filaments revealed an irregular dispersion, with the presence of holes and voids in the formulations, as the introduction of ceramic fillers in the LDPE matrix results in a heterogeneous system, and when an external load is applied, it induces the concentration of stresses and deformation mechanisms in the composite, initiating plastic deformation with separation of particles, causing the creation of holes and cavities. These defects are not harmful since the particles are transformed into solid bodies by diffusional atomic transport mechanisms, eliminating these defects in the sintering process. Printing of scaffolds by FFF was carried out without defects with a nozzle size of 1 mm. The TGA analysis identified a mass loss between 230 °C and 430 °C, with a* T_d *= 430 °C and* $T_{onset} \approx 250$ *°C for all formulations. The debinding and sintering process resulted in a resistant structure without cracks or defects at the interface between deposited filaments, with porosity internal and superficial parts and a dimensional contraction of around 30%.*

Keywords: *biomedical, scaffold, printing, composite.*

1. INTRODUCTION

The human body has about 40% of body mass responsible for sustaining the body's structural system, also comprising articular cartilage, bone tissue, and organs. These structures are susceptible to damage, injury, trauma, and degenerative diseases, requiring partial and/or total replacement in many cases. Thus, tissue engineering, through structures known as scaffolds, aims to replace these affected tissues and organs (Smoak and Mikos, 2020).

Scaffolds are a replacement alternative due to the ease of production and obtainment. They are three-dimensional structures obtained by additive manufacturing (AM) in the most diverse configurations according to the desired application, as well as presenting biocompatible, bioactive, and biodegradable properties, with a surface area that promotes cell adhesion and physical support, variables of paramount importance in the biomedical area. (Adithya et al., 2020).

One of the technologies within AM is fused filament manufacturing (FFF), in which viscous or molten material (filament) is extruded through a heated nozzle layer by layer, solidifying and creating precisely three-dimensional parts with dimensions of the order of 100 μm to 25 μm. An economical alternative with excellent production potential, it is considered one of the most used techniques worldwide (Sadaf et al., 2021).

Polymeric, metallic, composite materials, and ceramics such as alumina and zirconia are the main bets as raw materials for additive manufacturing due to the feasibility of printing, debinding, and sintering. Alumina and zirconia are high-density, inert bioceramics based on oxides and nitrides that, in addition to being mechanically stable, stand out for their biological properties, leading to relevant and innovative applications in the biomedical área (Ly et al., 2022).

Within this evaluation, this article aims to evaluate the obtainment of three-dimensional structures of ceramic scaffolds of alumina and zirconia by additive manufacturing through the study of parameters of printing, debinding, sintering, and mechanical properties.

2. BIOMATERIALS

Biomaterials characterize a fraction of the products used in the health area, being the first medical devices accepted for human use implanted between the mid-1940s and early 1950s, biomaterials are used for therapeutic and diagnostic purposes, healing or repair in a living organism (Agarwal et al., 2020), (Ratner et al., 2020).

Biomaterials are classified according to their origin, natural or synthetic, used in medical to come into contact with a biological system, whose purpose is an adequate, biocompatible response, repairing or replacing a given application when submitted to its host, without producing any harmful effect on tissue. One of the main applications of synthetic materials is for application in bone tissue (Ratner et al., 2020).

Human bone tissue performs various bodily functions, protects vital organs, and stores mineral compounds and cell production in the bone marrow. Currently, it is the second most transplanted tissue, and its repair is possible with bone tissue supplied directly from the patient or compatible donors (Collins et al., 2021).

As a biological material, composed of 50-70% organic constituents (hydroxyapatite), 20-40% organic constituents (collagen), 5-10% water, and 3% lipids, bone has a unique hierarchical structure with high resistance and fracture toughness. Its structure is divided into spongy/trabecular bone, with a porosity that varies from 50 to 90% in volume. The other structure located more externally is the cortical/compact bone, which has a porosity of less than 10%, structures capable of tolerating dynamic remodeling, maturation, and controlled resorption through osteoblastic cellular interactions responsible for new bone formation and osteoclastic, responsible for the resorption of old bone (Collins et al., 2021), (Li et al., 2021).

In addition, bone tissue is characterized by its self-healing abilities, but when the defect appears on a large scale, this self-healing can be disabled, delayed, and often not consolidated, requiring external intervention for its repair. With the need to satisfy these problems, the development of three-dimensional scaffolds is a way in which bone regeneration is possible with a combination of biomaterials, cells, and growth factors incorporated and even infiltrated, suppressing this deficient growth and improving in vivo functions (Marew and Birhanu, 2021).

3. SCAFFOLDS

The scaffolds are three-dimensional structures obtained by an additive manufacturing process from a combination of medical, magnetic resonance imaging, and computed tomography. Data studied directly from the patient's anatomy are recognized and converted to a 3D printer designed based on software for drawing and transforming digital signals into physical objects. Depending on the modeling required, it is possible to vary the type of material (polymer, ceramic, metal, composite), geometry, dimensions, mechanical properties, and porosity, obtaining a model that promotes tissue formation, growth, and cell proliferation when cultivated in vivo or in vitro (Cheng et al., 2021).

Scaffolds are developed to promote the regeneration of tissue that has gone through severe aesthetic problems and physical dysfunctions, defects due to natural causes, or a medical removal process. They must have the capacity to offer a space-time orientation and an architectural and biochemical structure for cells, present essential characteristics such as biological requirements, adequate structural characteristics, high porosity, and biomimetic components, allowing cells to infiltrate and adhere to their interconnected porous matrix (Ma et al., 2021).

3.1 Bioceramic materials used for the production of scaffolds

Ceramic biomaterials are a subclass of ceramics developed in the 1970s. They are characterized by excellent mechanical properties, biocompatibility, and bioactive potential, applied in medical joint implants, bone grafts, dental implants, hip implants, and scaffolds. Among the main ceramics used are bioinert (alumina and zirconia), bioactive (hydroxyapatite, bioglass, and glass-ceramic), and bioresorbable (tricalcium phosphate and gypsum) (Punj; Singh, 2022).

Alumina has biomedical applications due to its porosity above 90%, which allows cell growth in physiological environments, vascularization, cell migration, and liquid penetration in vivo applications, ensuring long-term resistance (Rosero-Alzate et al., 2021). It is classified as an inert, non-reactive, biocompatible bioceramic, applied to manufacture prosthetic implants and joint components, dental and orthopedic implants, body armor, tissue engineering, antioxidant coatings, and membranes (Grossin et al., 2021).

Introduced in the 1990s, zirconia is widely used in prosthetic dentistry due to its excellent biocompatibility properties, high mechanical strength, superior fatigue strength, high fracture resistance, Young's modulus, and chemical stability. Among the types of zirconia used in dentistry, we highlight partially stabilized zirconia doped with magnesium cation (Mg-PSZ), hardened alumina with zirconia (ZTA), and tetragonal zirconia polycrystals doped with yttrium cation (Y-TZP), being the main zirconia indicated due to the biomedical grade for being stabilized with 3% mol of yttria in order to maintain the desired mechanical properties (Ispas et al., 2021). Among the main applications of zirconia are biomedical, surgical, and dental implants (crowns, bridges, implants, and veneers), fuel cells, optical coatings, catalytic support, and sensors (Zhang; Wu; Shi, 2021).

3.2 Polymer matrix – additive for ceramic processing

Many materials are used and still studied for producing and modeling scaffolds, among which synthetic polymers such as low-density polyethylene (LDPE) stand out (Paleari et al., 2022).

LDPE is a polymer obtained by the polymerization of ethylene at high pressures, and its low density is related to the presence of a small number of branches. It is characterized by having a density between 0.910 – 0.94 $g.cm^{-3}$, easy processing, low tensile strength, high impact resistance, chemical resistance, flexibility even at low temperatures, high corrosion resistance, excellent electrical properties due to its thermal stability, good optical properties, and low toxicity. In the AM process, LDPE has disadvantages such as low strength and rigidity, low adhesion, and high shrinkage, which can result in defects during printing. On the other hand, some of these problems can be avoided when reinforced with metallic or ceramic particles in the production of composites, improving their storage modulus, increasing mechanical properties, and reducing shrinkage (Olesik et al., 2019).

Polymeric materials with a low melting point are the most used for the AM process due to their low cost, weight, and processing flexibility. Once reinforced with fibers, particles, or nanomaterials, they allow promising results to be obtained, developing new composite materials and enabling their use in scaffold applications (Faccio et al., 2021).

4. ADDITIVE MANUFACTURING - CAST FILAMENT MANUFACTURING

Fused Filament Manufacturing (FFF) is an additive manufacturing technique for complex parts developed in 1980. It is based on the use of continuous thermoplastic filaments, pulled by gears and melted through a heated nozzle that moves along the X-Y plane, deposited on a table that moves in the direction of the Z axis, producing the 3D part layer by layer that solidifies at room temperature (Mousapour et al., 2021.).

The FFF has proved very relevant in the most diverse fields, such as aerospace, medicine, biochemistry, electronics, the automotive industry, biotechnology, food, pharmaceuticals, equipment engineering, and chemical reactor projects. It is one of the most widespread techniques due to its economic advantages, versatile construction volumes and scales, and ability to co-print multiple compositions compatible with a wide range of materials. The filaments used can be modified with the addition of functional particles to improve the mechanical performance, and variations of printing nozzles can also be used; however, limitations of poor interfacial adhesion, high porosity, voids, interaction (bonding) between the fiber and the matrix and, between the load and the matrix, stress concentration and unsatisfactory sealing are still limitations of this technology (Tao et al., 2021).

In an FFF process where quality parts are produced without defects, the printing and machine parameters are essential due to the high impact on the characteristics obtained. Therefore, to meet the requested needs, the main effective process factors are the nozzle diameter, printing speed, construction orientation, scanning angle, layer thickness, filling pattern, extrusion temperature, and heated table (Solomon et al., 2021).

Based on these considerations, there is a need for an in-depth study on the development of ceramic composite scaffolds manufactured using the FFF technique, with the combination of inert materials of high hardness, such as alumina, and mechanical resistance, such as zirconia, to minimize and contribute to the problems observed in biomedical applications with greater efficiencies.

5. EXPERIMENT

5.1 Materials

Alumina A-1000SG (99.8%) from the company Almatis, with a particle size of 0.4 μm, with green density of 2.11 $g.cm^{-3}$ and density after sintering of 3.93 $g.cm^{-3}$ (supplier's data), and Zirconia TZ-3YS (99.8%) from the company Tosoh Corporation, with 3 mol% of Y_2O_3, particle size of 0.09 μm, green a density of 2.61 $g.cm^{-3}$ and density after sintering 6.05 $g.cm^{-3}$ (supplier's data). Low-density polyethylene (PEBD) Roto-K Natura from the company Karina Indústria e Comércio de Plásticos Ltda, supplied by the company Giroplastic, powder with a density of 0.937 $g.cm^{-3}$; Figure 1 describes the stages of the process carried out for the development of ceramic scaffolds. In stage A, the morphological characterization of the powders will be carried out, the formulations developed will be mixed, and the filaments will be produced using the extrusion process. In stage B, the scaffolds will be printed using the FFF technique, and stage C consists of debinding and sintering the scaffolds with the study of morphological and mechanical properties.

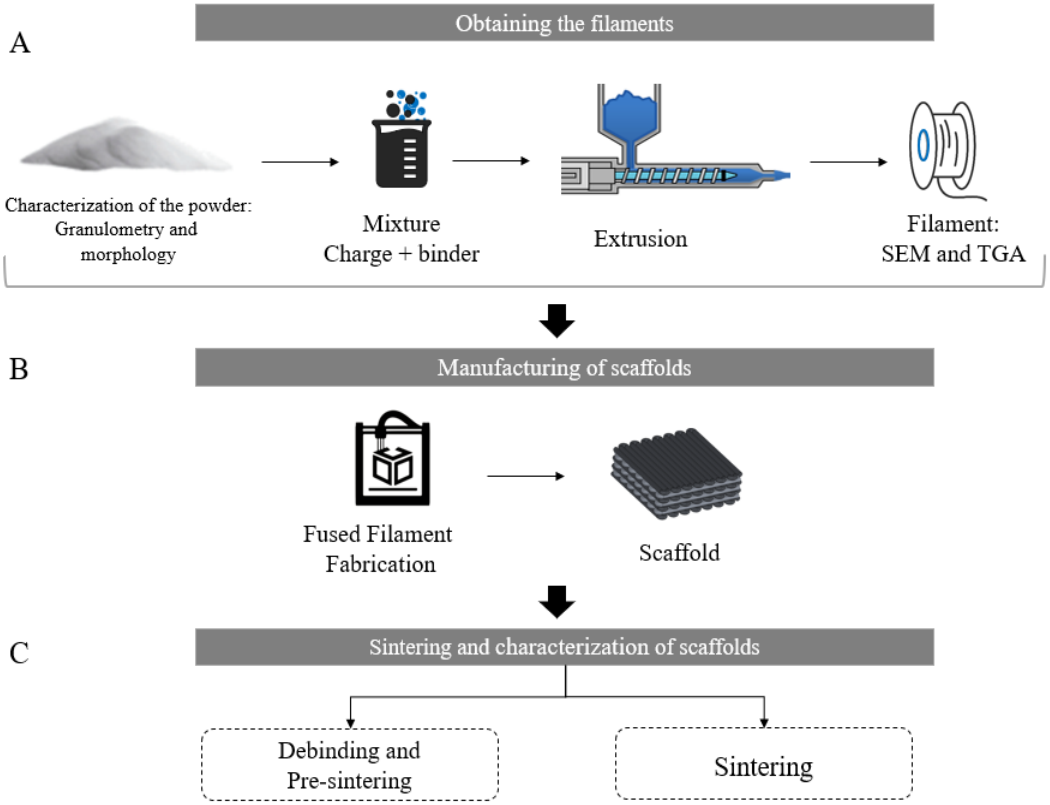

Figure 1. Schematic diagram of the study execution stages.

5.2 Methods

The morphology of the ceramic particles was evaluated by scanning electron microscopy in a field emission electron microscope (FEG-SEM) brand Tescan, model Mira3 (Czech Republic), with Energy Dispersion X-Ray Spectroscopy (EDS) system, brand Shimadzu, model SSX-550, operating at 10 kV accelerating voltage. The analysis was performed at Professor Israel Baumvol Central Microscopy Laboratory (LCMIC) at the University of Caxias do Sul.

The filaments were obtained using a twin-screw extruder, model ES 35 F-R Seibt, at the Polymer Laboratory of the University of Caxias do Sul (LPOL-UCS). The micrographs and distribution of the ceramic powders in the green filament were evaluated by FEG-SEM (LCMIC-UCS) in BSE mode (backscattered electrons) to highlight ceramic particles' contrast through the materials's atomic weight. The difference in the height of the invoiced surface was analyzed with the help of the OriginPro 9 software with the projection of color variation. This technique displays a single-band raster in which each pixel value is associated with a color, defining a set of values, with the blue color indicating the minimum surface and the red color the maximum height, visualized in each image microscopy. Chart 1 presents the codification and composition of the developed formulations.

Table 1. Coding of the developed formulations.

Code	Formulations (% wt)
PEBD/AL	45 % PEBD and 55 % alumina.
PEBD/ZR	45 % PEBD and 55 % zirconia.
PEBD/AL/ZR	45 % PEBD, 27.5 % alumina and 27.5% zirconia.

The scaffolds were obtained using the AE3D Wide 3D printer from AE3D Solutions in Print 3D, controlled by the Simplify3D® slicing software. The computational model was produced using the SolidWorks software and then saved in an SLT file compatible with the 3D printer programming. For printing the scaffolds, a nozzle size of 1 mm was used for all filaments, a table temperature of 60°C, an extruder temperature of 235°C to 240°C, and a printing speed of 15 mm/s. The standard three-dimensional geometry used for all scaffolds was 5 x 30 mm (height x side), filament spacing of 0.300 mm, and layer printing orientations 0°/45°, as shown in Figure 2.

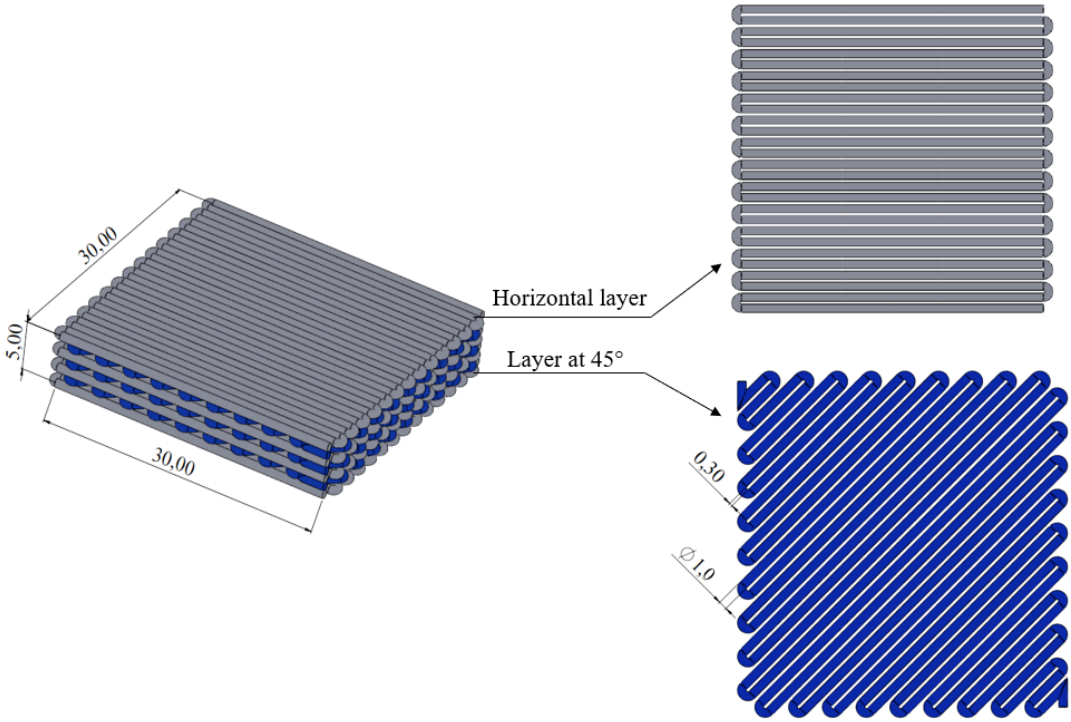

Figure 2. Three-dimensional geometry of scaffolds.

The debinding processes in a powder bed (wicking) and pre-sintering were carried out in a Sanchis furnace from the Laboratory of Ceramic Materials – UCS, with heating ramps according to the result obtained in thermogravimetric tests (TGA). After the debinding and pre-sintering process, the scaffolds are subjected to sintering at a rate of 1°C.min^{-1} at 1600°C, maintained for 2 hours, in a Lindberg oven.

6. RESULTS

The morphological analysis allowed identifying the difference in particle size of each ceramic, proving the compatibility of the data provided by the manufacturer, characterizing the alumina with particle sizes distributed between 0.4 – 0.6 µm and an irregular geometry and the zirconia with sizes of particles between 0.09 – 0.2 µm and a more spherical geometry, as shown in Figure 3.

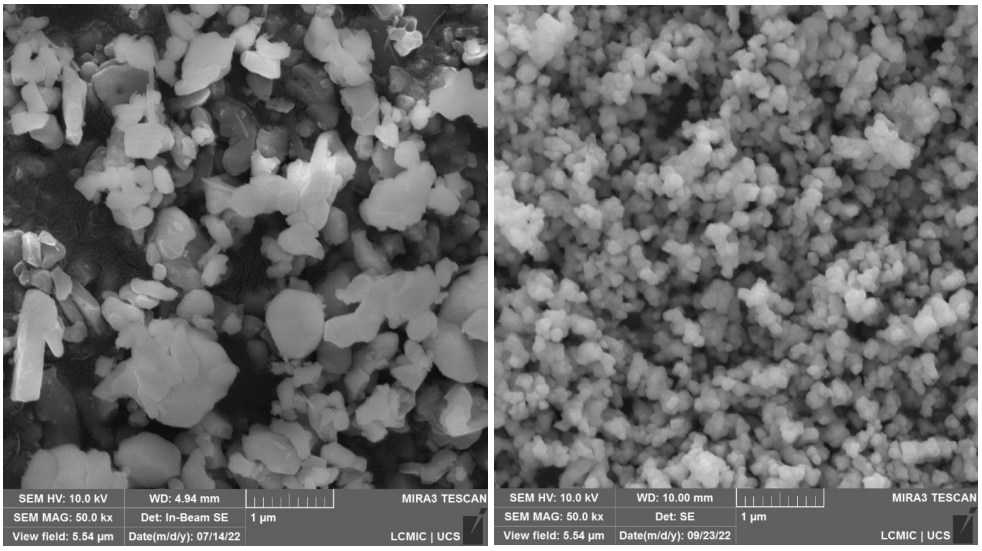

Figure 3. SEM micrographs of alumina (left) and zirconia powder (right) at 50,000x magnification.

The filaments obtained by extrusion did not show process defects, and no flaws were observed with the naked eye, presenting a smooth and malleable structure that allowed winding, obeying the standard diameter of 1.75 mm required for the printing process. The FEG-SEM analysis of the filaments after cryogenic fracture revealed the degree of dispersion of the particles in the polymeric binder, the internal imperfections of the filaments, the presence of pores, and the uniformity after extrusion, as seen in Figure 4.

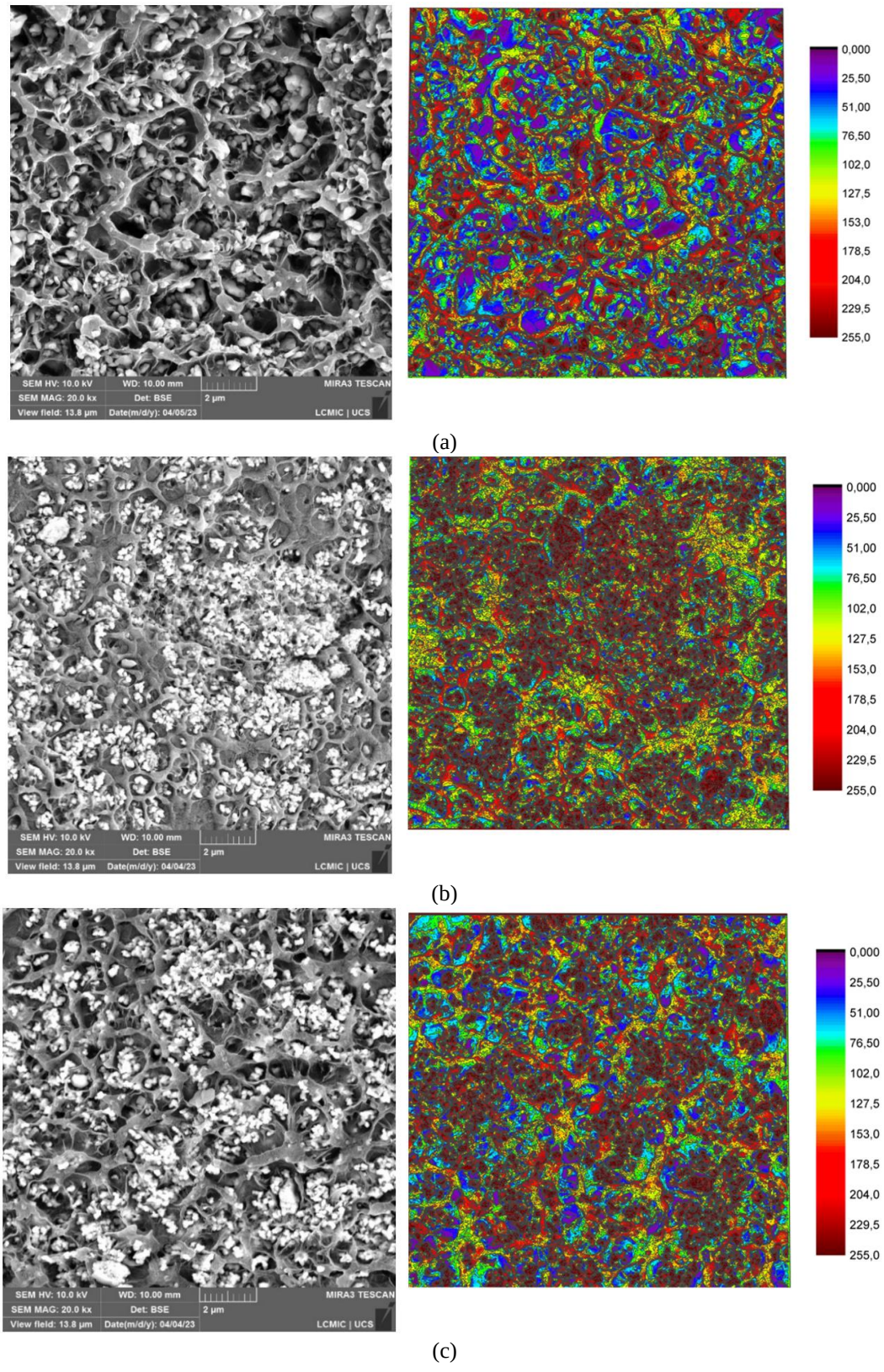

Figure 4. Micrographs of filaments with color map surface: (a) PEBD/AL, (b) PEBD/ZR and (c) PEBD/AL/ZR.

The micrographs in Figure 4 (a) – (c) revealed an irregular dispersion, with the presence of holes and voids in the formulations. The presence of this defect is related to the semicrystalline nature of LDPE when fractured, depending on the molecular and morphological characteristics induced by processing. The introduction of ceramic fillers into this matrix results in a heterogeneous system. When an external load is applied, it induces the concentration of stresses and deformation mechanisms in the composite, initiating plastic deformation with the separation of particles causing the creation of holes and cavities. These zones are stretched locally until rupture and are also identified by the difference in the height of the fractured surface with the color projection on a color map surface graph of each filament, demonstrating the greatest variation for mixtures with the binder. Due to LDPE's low polarity and surface free energy, interfacial adhesion is weak, causing separation of the matrix-filler interface, which is visibly identified by the micrographs presented (Arencón; Velasco, 2009). Furthermore, with plastic deformation applied during fracture, these voids tend to grow in the direction of stress, forming dimple-shaped holes within the filling phase around the particles, resulting in a more ductile fracture with adhesive failure between the matrix and particles (interfacial detachment). These defects, evident in LDPE mixtures, tend not to be harmful since, in the sintering process, the particles are transformed into solid bodies by diffusional atomic transport mechanisms, acquiring mechanical resistance (Awaja et al., 2016).

It is also possible to identify the presence of small agglomerates in samples containing zirconia, characteristic of their particle size < 0.2 μm, which are not accentuated. In the composite mixing process, particles tend to agglomerate when the % by weight ratio is increased, causing a non-uniform distribution with larger particle sizes. Considerably, the size of the powders can significantly affect the filament flexibility and rigidity, viscosity, surface roughness, reactivity, and wettability with the binder for the resolution of the printed product; therefore, typical particle sizes used should not exceed the range of 0.3 to 0.8 mm, being thin enough to avoid clogging the printing nozzle (Mocanu et al., 2022).

The scaffolds were printed satisfactorily, obeying the proposed cubic dimensions according to the literature, considering porosity, one of the most important variables for producing scaffolds. According to Collins et al. (2021), an ideal working range of pore size is 100 μm to 900 μm for application in bone tissue due to the sufficient space provided for nutrient and oxygen supply, vascularization, permeabilization, cell growth, and better interaction for the formation of the new fabric. Figure 5 shows the scaffolds printed by FFF.

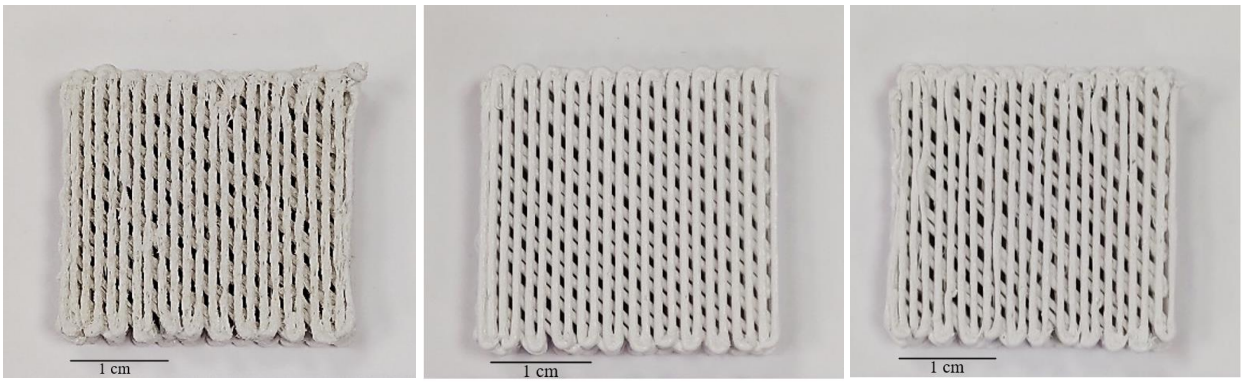

(a) (b) (c)

Figure 5. Scaffolds produced by 3D printing: (a) PEBD/AL, (b) PEBD/ZR, and (c) PEBD/AL/ZR.

The stage of extracting the organic binder or debinding process occurs by degradation or fusion, with its removal through the porous medium formed by the body by diffusion or permeation. TGA/DTG analysis of the filaments after printing (Figure 6-a) made it possible to evaluate the degradation temperature (T_d) of the material for the construction of the heating ramp based on literature analysis (Sadaf et al., 2021). It was possible to observe from the TGA graph a loss of mass between 230 °C and 430 °C, with T_d = 430 °C and $T_{onset} \approx 250$ °C. In these regions observed with high mass loss rates, a longer residence time in the oven was defined at temperatures prior to T_d and T_{onset}, with 600 min (10 h) of isotherm at 200 °C and 390 °C and around 120 min at 450 °C so that a gradual removal of the binder could be achieved, since the sudden evaporation means that the exit path through the pores does not form, causing the part to lose its integrity, or even promote swelling due to the trapped gas formed by polymer decomposition (Enneti et al., 2012). The heating ramp is shown in Figure 6 (b), used for the developed formulations.

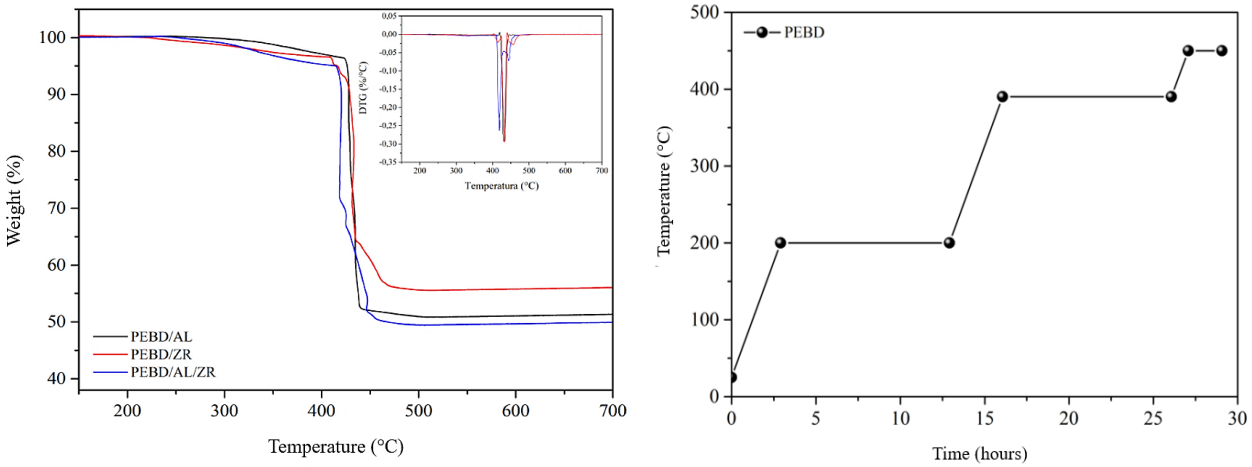

(a) (b)

Figure 6. Binder extraction stage: (a) TGA/DTG of the filaments and (b) heating ramp for debinding the scaffolds.

After sintering the scaffolds (Figure 7), it was possible to identify the dimensional reduction in the thickness of the layers and filaments and the porosity, with a dimensional contraction between 25% and 30% for all formulations. No scaffold presented defects such as cracks on the surface nor interface defects between deposited filaments, characterizing an adequate printing process with a union between layers at the time of deposition of the molten and solidified filament. The increased pore size allows greater permeability and bone growth due to the space provided, enabling cell-structure interaction and diffusion of oxygen and nutrients (Collins et al., 2021).

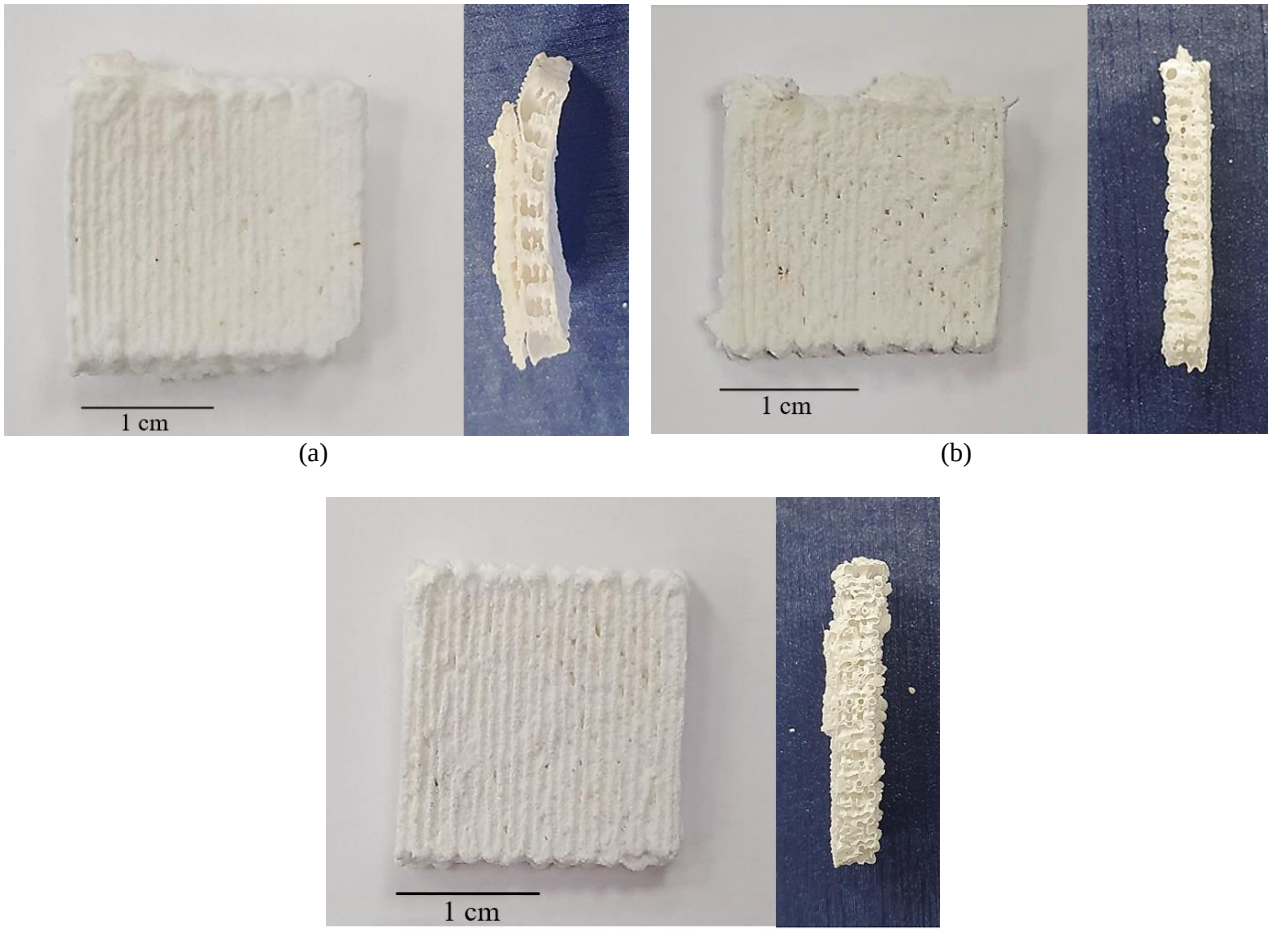

(a) (b)

(c)

Figure 7. Sintered scaffolds and respective cutting sections: (a) PEBD/AL, (b) PEBD/ZR, and (c) PEBD/AL/ZR.

It is important to highlight that the combination of ceramic composite materials to obtain scaffolds promotes the regeneration and formation of damaged tissue with bioactive and biocompatible properties with efficient results that can be applied without damaging the integrity of the host, which could result in clinical failure. This is summarized in the structural characteristics of bone tissue, which presents high resistance and fracture toughness, contributing to the need to develop compatible three-dimensional structures that allow mimicking the damaged tissue with a bioactive purpose, promoting the adhesion of the implant to the bone, assisting in repair, and collaborating with growth in the biomedical field.

Therefore, this research aimed to expand knowledge in using alternative composite materials with biological characteristics, establishing a solution to minimize the problems observed in biomedical applications and contributing to this system being a viable, compatible, and promising operation for desired applications.

7. ACKNOWLEDGEMENTS

We want to thank the University of Caxias do Sul for providing the laboratories and equipment for obtaining and manufacturing the filaments, printing the parts, and furnaces for the debinding and sintering processes. CAPES funded this work under grant number 88887.819444/2023-00.

8. REFERENCES

Adithya, S. P., Sidharthan, D. S., Abhinandan, R., Balagangadharan, K. and Selvamurugan, N., 2020. "Nanosheets-incorporated bio-composites containing natural and synthetic polymers/ceramics for bone tissue engineering", *International Journal of Biological Macromolecules*, Vol. 164, p. 1960–1972.

Agarwal, K.M., Singh, P., Mohan, U., Mandal, S. and Bhatia, D., 2020. "Comprehensive study related to advancement in biomaterials for medical applications", *Sensors International*, Vol. 1, p. 100055.

Arencón, D. and Velasco, J.I., 2009. "Fracture toughness of polypropylene-based particulate composites", *Materials*, Vol. 2, n. 4, p. 2046–2094.

Awaja, F., Zhang, S., Tripathi, M., Nikiforov, A. and Pugno, N., 2016. "Cracks, microcracks and fracture in polymer structures: Formation, detection, autonomic repair", *Progress in Materials Science*, Vol. 83, p. 536–573.

Balakrishnan, S. B., Kuppu, S. and Thambusamy, S., 2021. "Biologically important alumina nanoparticles modified polyvinylpyrrolidone scaffolds *in vitro* characterizations and it is *in vivo* wound healing efficacy", *Journal of Molecular Structure*, Vol. 1246, p. 131195.

Cheng, L., Suresh, S.K., He, H., Rajput, R.S., Feng, Q., Ramesh, S., Wang, Y., Krishnan, S., Ostrovidov, S., Camci-Unal, G. and Ramalingam, M., 2023. "3D printing of micro-and nanoscale bone substitutes: a review on technical and translational perspectives", *International Journal Nanomedicine*, Vol. 16, p. 4289–4319.

Collins, M.N., Ren, G., Young, K., Pina, S., Reis, R.L. and e Oliveira, J.M., 2021. "Scaffold fabrication technologies and structure/function properties in bone tissue engineering", *Advanced Functional Materials*, Vol. 31, nº 21.

Enneti, R.K., Park, S.J., German, R.M. and Atre, S.V., 2012. "Review: Thermal debinding process in particulate materials processing", *Materials and Manufacturing Processes*, Vol. 27, p. 103–118.

Faccio, M., Catafesta, J. and Zorzi, J.E., 2021. "Aditivos para fabricação por manufatura aditiva de pós-cerâmicos pela técnica de filamento fundido: uma breve revisão", *Revista Tecnologia*, Vol. 42, n. 1, p. 1–12.

Grossin, D., Montón, A., Navarrete-Segado, P., Özmen, E., Urruth, G., Maury, F., Maury, D., França, C., Tourbin, M., Lenormand, P. and Bertrand, G., 2021. "A review of additive manufacturing of ceramics by powder bed selective laser processing (sintering/melting): Calcium phosphate, silicon carbide, zirconia, alumina, and their composites", *Open Ceramics*, Vol. 5, n° 100073, p. 1–21.

Hermouet, F., Rogaume, T., Guillaume, E., Richard, F., Marquis, D. and Ponticq, X., 2021. "Experimental characterization of the reaction-to-fire of an Acrylonitrile-Butadiene-Styrene (ABS) material using controlled atmosphere cone calorimeter", *Fire Safety Journal*, Vol. 121, nº 103291, p. 1–17.

Ispas, A., Iosif, L., Murariu-Măgureanu, C., Craciun, A. and Constantiniuc, M., 2021. "Zirconia in dental medicine: a brief overview of its properties and processing techniques", *Human & Veterinary Medicine. International Journal of the Bioflux Society*, Vol. 13, nº 1, p. 33–39.

Li, Y., Liu, Y., Li, R., Bai, H., Zhu, Z., Zhu, L., Zhu, C., Che, Z., Liu, H., Wang, J. and Huang, L., 2021. "Collagen-based biomaterials for bone tissue engineering", *Materials & Design*, Vol. 210, p. 110049.

Ly, M., Spinelli, S., Hays, S. and Zhu, D., 2022. "3D Printing of Ceramic Biomaterials", *Engineered Regeneration*, Vol. 3, nº 1, p. 41–52.

Ma, P., Wu, W., Wei, Y., Ren, L., Lin, S. and Wu, J., 2021. "Biomimetic gelatin/chitosan/polyvinyl alcohol/nano-hydroxyapatite scaffolds for bone tissue engineering", *Materials & Desing*, Vol. 207, p. 109865.

Marew, T. and Birhanu, G., 2021. "Three dimensional printed nanostructure biomaterials for bone tissue engineering", *Regenerative Therapy*, Vol. 18, p. 102–111.

Mocanu, A. C., Miculescu, F., Dascălu, C., Voicu, S.I., Pandele, M., Ciocoiu, R., Batalu, D., Dondea, S., Mitran, V. and Ciocan, L., 2022. "Influence of Ceramic Particles Size and Ratio on Surface—Volume Features of the Naturally

Derived HA-Reinforced Filaments for Biomedical Applications", *Journal of Functional Biomaterials*, Vol. 13, n. 4, p. 1–19.

Mousapour, M., Salmi, M., Klemettinen, L. and Partanen, J., 2021. "Feasibility study of producing multi-metal parts by fused filament fabrication (FFF) technique", *Journal of Manufacturing Processes*, Vol. 67, p. 438–446.

Olesik, P., Godzierz, M. and Kozioł, M., 2019. "Preliminary Characterization of Novel LDPE-Based Wear-Resistant Composite Suitable for FDM 3D Printing", *Materials*, Vol. 12, p. 1–19.

Paleari, L., Bragalia, M., Mariani, M. and Nanni, F., 2022. "Acrylonitrile butadiene styrene – carbon nanotubes nanocomposites for 3D printing of health monitoring components", *Journal of Reinforced Plastics & Composites*, Vol 0, p. 1–14.

Punj, S., Singh, J. and Singh, K., 2022. "Ceramic biomaterials: Properties, state of the art and future prospectives", *Ceramics International*, Vol. 47, nº 20, p. 1–16.

Ratner, B.D., Hoffman, A.S., Schoen, F.J., Lemons, J.E., Wagner, W.R., Sakiyma-Elbert, S.E., Zhang, G. and Yaszemski, M.J., 2020. "Introduction to biomaterials science: an evolving, multidisciplinary endeavor", *Biomaterials Science*, Fourth Edi. Elsevier, p. 3–19.

Rosero-Alzate, É. L., Zapata-Pernett, M.A., Vega-Ortiz, D., Puerta-Tinoco, L.D., Múnera-Ramírez, M.C., Esguerra-Arce, J. and Esguerra-Arce, A., 2021. "Influence of porosity on the biomimetic growing patterns of bone-like apatite on the surface of calcium phosphate – calcium titanate – alumina compounds", *DYNA (Colombia)*, Vol. 88, nº 218, p. 24–33.

Sadaf, M., Bragaglia, M. and Nanni, F., 2021. "A simple route for additive manufacturing of 316L stainless steel via fused filament fabrication", *Journal of Manufacturing Processes*, Vol. 67, p. 141–150.

Sakthiabirami, K., Kang, J., Jang, J., Soundharrajan, V., Lim, H., Yun, K.,Park, C., Lee, B., Yang, Y. and Park, S., 2021. "Hybrid porous zirconia scaffolds fabricated using additive manufacturing for bone tissue engineering applications", *Materials Science & Engineering C*, Vol 123, p. 111950.

Smoak, M. M., and Mikos, A. G., 2020. "Advances in biomaterials for skeletal muscle engineering and obstacles still to overcome", *Materials Today Bio*, Vol. 7, p. 100069.

Solomon, I.J., Sevvel, P. and Gunasekaran, J., 2021. "A review on the various processing parameters in FDM", *Materials Today Proceedings*, Vol. 37, Part 2, p. 509–514.

Spirandeli, B.R., Ribas, R.G., Amaral, S.S., Martins, E.F., Esposito, E., Vasconcellos, L.M.R., Campos, T.M.B., Thim, G.P. and Trichês, E.S., 2021. "Incorporation of 45S5 bioglass via sol-gel in β-TCP scaffolds: Bioactivity and antimicrobial activity evaluation", *Materials Science and Engineering C*, Vol. 131, nº 112453, p. 1–12.

Tao, Y., Kong, F., Li, Z., Zhang, J., Zhao, X., Yin, Q., Xing, D. and Li, P., 2021. "A review on voids of 3D printed parts by fused filament fabrication", *Journal of Materials Research and Technology*, Vol. 15, p. 4860–4879.

Zhang, X.; Wu, X.; Shi, J., 2021. "Additive manufacturing of zirconia ceramics: a state-of-the-art review", *Journal of Materials Research and Technology*, Vol. 9, n°. 4, p. 9029–9048.

9. RESPONSIBILITY NOTICE

The authors are the only responsible for the printed material included in this paper.